

## ***Electronic Supplementary Information (ESI)***

### **Enhanced capacitive deionization of graphene/mesoporous carbon composites**

Dengsong Zhang,<sup>\*a</sup> Xiaoru Wen,<sup>a</sup> Liyi Shi,<sup>\*b</sup> Tingting Yan<sup>a</sup> and Jianping Zhang<sup>b</sup>

<sup>a</sup> *Research Center of Nano Science and Technology, Shanghai University, Shanghai 200444, China.*

*Fax: 86 21 66134852; E-mail: dszhang@shu.edu.cn*

<sup>b</sup> *Department of Chemistry, Shanghai University, Shanghai 200444, China. Fax: 86 21 66136038;*

*E-mail: shiliyi@shu.edu.cn*

#### **Experimental section**

##### **Preparation of the materials**

Triblock copolymers Pluronic F127 ( $M_w=12600$ , PEO<sub>106</sub>-PPO<sub>70</sub>-PEO<sub>106</sub>) was purchased from Acros Corp. Other chemicals were supplied by Sinopharm Chemical Reagent Company. All the reagents were used without any purification and deionized (DI) water was used in all experiments. Graphite oxide (GO) was produced from natural graphite powders according to a procedure reported previously<sup>1</sup> with some modifications.

Typically, after graphite powders (3.0 g) being placed in a concentrated H<sub>2</sub>SO<sub>4</sub> (98 %, 120 mL) at 0 °C, KMnO<sub>4</sub> (15 g) was added gradually under continuous stirring. The mixture was kept at 35 °C for 2.5 h and then diluted gradually with 250 mL of DI water in an ice-water bath followed by re-dilution with the mixed solution containing 250 mL of DI water and 20 mL of H<sub>2</sub>O<sub>2</sub> (30 %). Finally, the mixture was filtered, washed with a 5 wt% HCl aqueous solution and DI water until

sulfate could not be detected with  $\text{Ba}(\text{NO}_3)_2$ . The dried GO was obtained by a vacuum evaporation at 45 °C. In addition, GE nanosheets were produced by the thermal exfoliation of the prepared GO at 300 °C for 5 min under the air atmosphere as described elsewhere<sup>2</sup>.

A series of GE/MC composites were prepared by using triblock copolymer F127 as a template and resol as a carbon precursor via a direct triblock-copolymer-templating method in the presence of GE. The synthesis of resol was based on a procedure reported previously<sup>3,4</sup> and the molar ratio of phenol, formaldehyde, NaOH and F127 was kept at 1:2:0.1:0.010-0.015. In addition, the weight percentage of GE in the composites was varied by 1 wt.%, 5 wt.%, 10 wt.%, and 15 wt.%. In a typical preparation, 5.0 g of resol precursors in ethanol solution containing 0.61 g of phenol and 0.39 g of formaldehyde was added into the transparent mixed solution composed of 1.0 g of F127 and 25.3 mL of ethanol, and then the solution was stirred for 30 min. Subsequently, a GE suspension obtained by the sonication in 12.7 mL of ethanol for 30 min was added into the above as-prepared mixed solution. Finally, a homogeneous solution was acquired after stirring for 30 min followed by sonication for 30 min. The resultant solution was poured into dishes to evaporate ethanol at 35 °C for 8 h followed by heating at 120 °C for 24 h. The carbonization of the as-made products was completed at 400 °C for 2 h and 600 °C for 4 h under a  $\text{N}_2$  atmosphere with a flow rate of 85  $\text{cm}^3/\text{min}$  and a heating rate of 1 °C /min. Finally, the prepared samples were denoted as GE-1%/MC, GE-5%/MC, GE-10%/MC, and GE-15%/MC, respectively.

The electrodes were prepared as follows. A mixture of the active material, acetylene black, and polytetrafluoroethylene with a weight ratio of 80:15:5 was ground together to form a homogeneous slurry. Finally, the mixed slurry was coated onto the graphite paper substrate and

then dried at 110 °C for 12 h.

### General characterization

The morphology of the samples was observed by transmission electron microscopy (TEM, JEOL JEM-200 CX). The X-ray diffraction (XRD) measurements were performed with Rigaku D/MAX-RB X-ray diffractometer by using Cu K $\alpha$  (40 kV, 20 mA) radiation and a secondary beam graphite monochromator. Nitrogen adsorption-desorption measurements were performed at 77 K with a Micromeritics ASAP2020 instrument. Prior to the measurements, the samples were degassed overnight at 493 K in a vacuum line. The specific surface area and pore volume were calculated with Brunauer- Emmett- Teller (BET) method and the pore size distribution was estimated with desorption branches based on Barrett- Joyneer- Halenda (BJH) model.

### Electrochemical measurements

The electrochemical measurements were conducted in a three-electrode cell in which the prepared electrode, a graphite sheet, and a saturated calomel electrode (SCE) acted as the working, counter and reference electrodes, respectively. All the experiments were carried out at the room temperature.

The cyclic voltammetry (CV) measurements were carried out on the CHI-660D electrochemical workstation with a potential range from -0.5 to 0.5 V. The specific capacitance ( $C_m$ ) at a given rate  $\nu$ , were calculated from voltammetric response using the following equations<sup>5</sup> :

$$C_m = Q / (2 m \Delta V) \quad (S1)$$

Where  $m$  is the mass of the activated substance,  $\Delta V$  is the range of potential, and  $Q$  is the integrated area of CV curve, respectively.

The electrochemical impedance spectroscopy (EIS) measurements were also conducted using the CHI-660D electrochemical workstation in a frequency range from 10 mHz to 10 kHz. The amplitude of the alternating voltage was 5 mV around the equilibrium potential (0 V).

The galvanostatic charge-discharge (GC) measurements were conducted using an automatic LAND battery test instrument to evaluate the charge/discharge performance in a 0.5 M NaCl aqueous solution. The capacitance was calculated using the following equation<sup>6</sup>.

$$C_g = (I \times \Delta t) / \Delta V \quad (\text{S2})$$

Where  $C_g$  is the capacitance,  $I$  is the constant discharge current,  $\Delta t$  is the discharge time and  $\Delta V$  is the potential change during discharge excluding the portion of  $iR$  drop.

## Discussion

With the purpose of demonstrating a successful exfoliation process, a wide-angle XRD characterization of the GO was conducted. As clearly seen in Fig. S1A, a strong diffraction peak centered at about  $10^\circ$  can be found for GO, together with the disappearance of graphite peak between  $25^\circ$  and  $30^\circ$ , suggesting the complete oxide of the graphite. Obviously, the XRD pattern of pristine GE prepared by a low thermal exfoliation indicates an amorphous structure<sup>7, 8</sup>, which is the characteristic of disordered and exfoliated GE<sup>1</sup>. Wrinkled paper-like GE proved by the TEM image (as seen in Fig. S2) further demonstrates a successful exfoliation process, in consistent with the result reported previously<sup>2</sup>. In addition, the GE/MC composite with various content GE show two similar weak shoulder and broad diffraction peaks, which can be indexed to (002) and (100) diffractions for a typical graphite carbon<sup>9</sup> as illustrated in the inset of Fig. S1A. However, the intensities of relative peaks increase gradually related to an improved graphitic crystallinity of the composites along with a slight shift toward high-angles with the increasing content of GE. The

result demonstrates that the GE has been successfully introduced and it makes no obvious difference to the structure of MC.

Generally, the peak appeared below  $1^\circ$  in the small-angle XRD is indexed as (100) diffraction, associated with 100 reflections of two-dimensional (2D) hexagonal symmetry<sup>10</sup>. As expected, clearly seen in Fig S1B, highly ordered mesoporous structure is formed via a self-assembly of the triblock copolymer for MC. Noteworthy, the GE/MC composites display similar diffraction peaks in spite of the decrease of the intensity. So it can be deduced that ordered mesoporous channels retain well after the addition of GE. The MC with high surface area and easily accessible pore structure in combination with highly conductive GE meets the requirements of CDI electrodes.

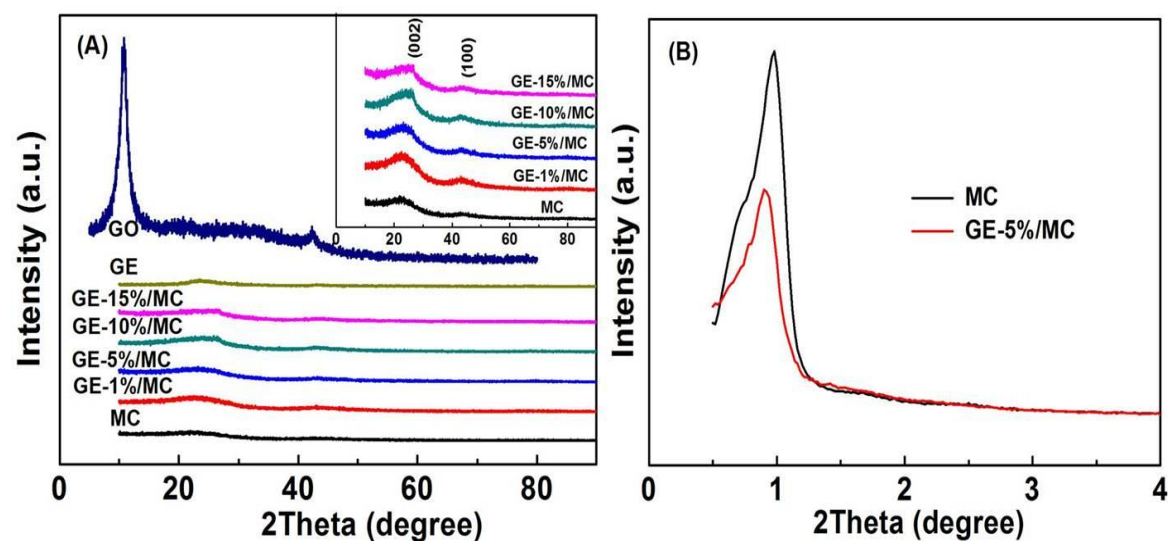


Fig. S1 (A) wide angle and (B) small angle XRD patterns of the prepared materials. The inset of (A) is the enlarged XRD patterns.

As seen in Fig. S3, the pristine GE prepared from a low-temperature thermal exfoliation of GO also displays a hysteresis loop similar to Type IV, which is characteristic of mesoporous structures mainly resulting from the overlapped regions created by the folded and crumpled GE sheets<sup>11</sup>.

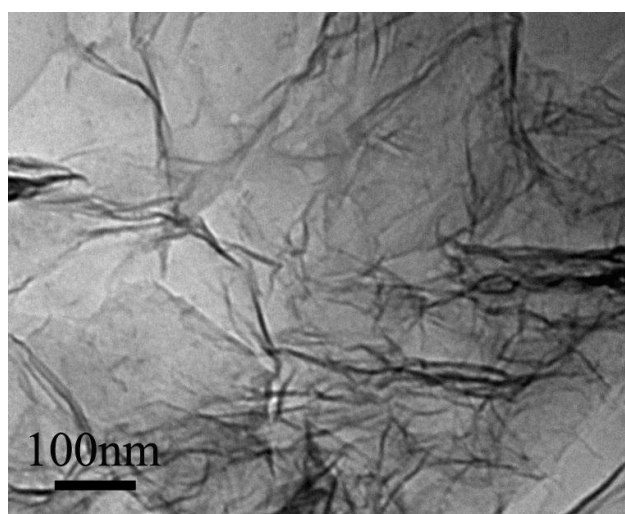


Fig. S2 TEM image of the prepared GE.

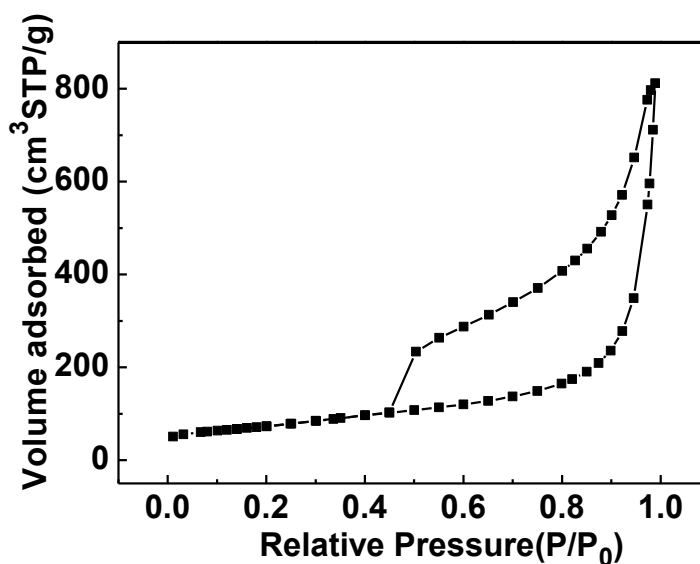


Fig. S3 Nitrogen adsorption-desorption isotherm of the prepared GE.

The CV curves obtained at a scan rate from 1 to 10 mV/s in a 0.5 M NaCl aqueous solution by using GE/MC electrodes for comparison are shown in Fig. S4. Achieving rectangular-shaped CV profiles over a wide range of scan rates is the ultimate goal and this behavior is important for practical applications involving high energy and power density<sup>12</sup>. As depicted in Fig. S4, all the CV curves at various rates exhibit typical capacitor-like characteristics with symmetric cyclic shapes, which indicate that electro sorption charge /discharge is a reliable and highly reversible process<sup>13</sup>. At a relatively low scan rate such as 1 or 2 mV/s, a more rectangular shape can be observed, as pointed by Xing et al that the ions have enough time to diffuse into the inner surface

of mesoporous channels at a low scan rate<sup>14</sup>. However, when the scan rate increases to 5 or 10 mV/s, the rectangle shape is slightly distortional. These imply that at relatively high rates the ohmic resistances for ion motion in the pores have affected the double layer formation mechanism<sup>15</sup>. In addition, the increasing current respond resulting from corresponding scan rate has enhanced the differences of potential between the mouth and bottom of the pore, which will lead to a delayed current response<sup>16</sup>.

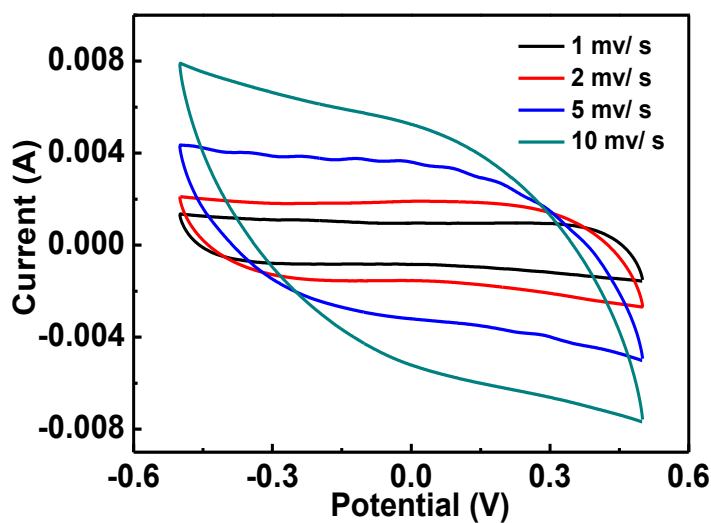


Fig. S4 CV profiles of the GE/MC composite electrode in a 0.5 M NaCl aqueous solution at various scan rates.

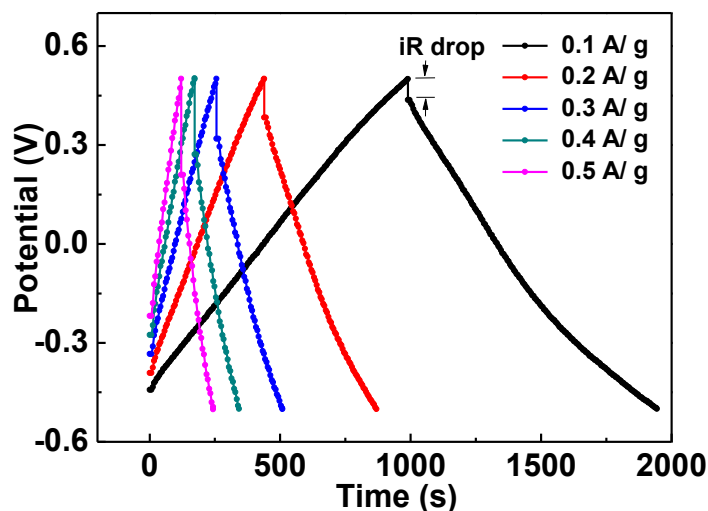


Fig. S5 Galvanostatic charge/discharge curves of the GE/MC composite electrode in a 0.5 M NaCl aqueous solution at various current loads.

The cell was cycled at different current densities within a potential window (-0.5 - 0.5 V) and the results were presented in Fig. S5. As observed, with a low current density the voltage response is closer to an ideal linear charge/voltage relationship, indicating that a lower iR drop (potential drop) is obtained. Here, the iR drop of the capacitor results mainly from the entire resistance of the cell containing the solution resistance, electrode resistance, and also ion migration resistance<sup>17</sup> and lower resistance is beneficial for high performance CDI process. What's more, the iR drop is increasing with the increasing current density, associated with the above mentioned resistance of the cell.

Table S1 Surface texture properties and the specific capacitance obtained in a 0.5 M NaCl aqueous solution at a scan rate of 5 mV/s of the prepared GE.

	$S_{\text{BET}}$ (m <sup>2</sup> /g)	$V_{\text{BJH}}$ (cm <sup>3</sup> /g)	$D_{\text{Pore}}$ (nm)	$C_{\text{m}}$ (F/g)
GE	259.8	0.85	13.0	43.33

#### References:

1. H. X. Chang, G. F. Wang, A. Yang, X. M. Tao, X. Q. Liu, Y. D. Shen and Z. J. Zheng, *Adv. Funct. Mater.*, 2010, **20**, 2893-2902.
2. Q. L. Du, M. B. Zheng, L. F. Zhang, Y. W. Wang, J. H. Chen, L. P. Xue, W. J. Dai, G. B. Ji and J. M. Cao, *Electrochim. Acta*, 2010, **55**, 3897-3903.
3. Y. Meng, D. Gu, F. Q. Zhang, Y. F. Shi, L. Cheng, D. Feng, Z. X. Wu, Z. X. Chen, Y. Wan, A. Stein and D. Y. Zhao, *Chem. Mater.*, 2006, **18**, 4447-4464.
4. Y. Meng, D. Gu, F. Q. Zhang, Y. F. Shi, H. F. Yang, Z. Li, C. Z. Yu, B. Tu and D. Y. Zhao, *Angew. Chem. Int. Edit.*, 2005, **44**, 7053-7059.
5. J. Feng, J. Zhao, B. Tang, P. Liu and J. Xu, *J. Solid State Chem.*, 2010, **183**, 2932-2936.
6. D. Y. Qu and H. Shi, *J. Power Sources*, 1998, **74**, 99-107.
7. M. J. McAllister, J. L. Li, D. H. Adamson, H. C. Schniepp, A. A. Abdala, J. Liu, M. Herrera-Alonso, D. L. Milius, R. Car, R. K. Prud'homme and I. A. Aksay, *Chem. Mater.*, 2007, **19**, 4396-4404.
8. R. Verdejo, F. Barroso-Bujans, M. A. Rodriguez-Perez, J. A. de Saja and M. A. Lopez-Manchado, *J. Mater. Chem.*, 2008, **18**, 2221-2226.
9. H. F. Yang, Y. Yan, Y. Liu, F. Q. Zhang, R. Y. Zhang, Y. Meng, M. Li, S. H. Xie, B. Tu and D. Y. Zhao, *J. Phys. Chem. B*, 2004, **108**, 17320-17328.
10. G. L. Xu, S. R. Chen, J. T. Li, F. H. Ke, L. Huang and S. G. Sun, *J. Electroanal. Chem.*, 2011, **656**, 185-191.
11. Z. B. Lei, N. Christov and X. S. Zhao, *Energy & Environmental Science*, 2011, **4**, 1866-1873.
12. S. R. S. Prabaharan, R. Vimala and Z. Zainal, *J. Power Sources*, 2006, **161**, 730-736.
13. L. D. Zou, L. X. Li, H. H. Song and G. Morris, *Water Res.*, 2008, **42**, 2340-2348.
14. W. Xing, S. Z. Qiao, R. G. Ding, F. Li, G. Q. Lu, Z. F. Yan and H. M. Cheng, *Carbon*, 2006, **44**, 216-224.

15. H. Y. Liu, K. P. Wang and H. S. Teng, *Carbon*, 2005, **43**, 559-566.
16. L. X. Li, L. D. Zou, H. H. Song and G. Morris, *Carbon*, 2009, **47**, 775-781.
17. Y. R. Lin and H. Teng, *Carbon*, 2003, **41**, 2865-2871.